

Electronic Supplementary Information for

**A material of hierarchical interlayer-expanded MoS₂
nanosheets/hollow N-doped carbon nanofibers as a
promising Li⁺/Mg²⁺ co-intercalation host**

*Xianbo Yu,^a Guangyu Zhao,^{*ab} Chao Liu,^a Huihuang Huang,^a Xiaojie Shen,^a and
Naiqing Zhang^{*ab}*

^aState Key Laboratory of Urban Water Resource and Environment, School of Chemistry and Chemical Engineering, Harbin Institute of Technology, Harbin 150001, China

^bAcademy of Fundamental and Interdisciplinary Sciences, Harbin Institute of Technology, Harbin 150001, China.

E-mail: zhaogy810525@gmail.com; znqmw@163.com

Experimental Section

Chemicals. Molybdenum trioxide (MoO₃, 99.5%), imidazole (C₃H₄N₂, 99.5%), pyrrole (Py, 99.7%), thiourea (CH₄N₂S, 99.0%), absolute ethanol (C₂H₅OH, 99.9%) were purchase from Shanghai Aladdin biochemical technology co., LTD (China). All the chemicals were used without further purification.

Preparation of Mo-MOFs and Mo-MOFs@PPy. The Mo-MOFs was synthesized by a facile hydrothermal method. Simply, 3.5 g of MoO₃ was dispersed in 250 mL of distilled water and after sonication for 20 min, 1.66 g of imidazole was added into the mixture solution. Then the resultant solution was kept at 70°C for 10 h under continuous stirring, and the white precipitates were collected and washed by suction filtration with distilled water and dried through a freeze-drying process. As for Mo-MOFs@PPy, the 250 mg of Mo-MOFs was firstly dissolved in the 50 mL of distilled water, and then 400

mg of $\text{FeCl}_3 \cdot 6\text{H}_2\text{O}$ was dispersed in the above solution. After stirring for 10 min, the 300 μL of pyrrole added slowly to the solution and continuous stirred for another 4 h at room temperature. At last, the black solid products were collected by centrifuged and washed with absolute ethanol and distilled water and then dried through a freeze-drying process.

Preparation of O-MoS₂/HN-CNFs, P-MoS₂/HN-CNFs, and O-MoS₂/N-C.

Typically, the O-MoS₂/HN-CNFs was synthesized as follows. First, the as-prepared Mo-MOFs@PPy was performed by thermal treatment in a furnace at 400°C for 1 h under Ar flow. After cooling to room temperature, the Mo-precursor was obtained. Second, 100 mg of Mo-precursor was dissolved in 60 mL mixture solution (36 mL absolute ethanol and 24 mL distilled water), and then 760 mg of thiourea was added. After stirring for 20 min, the obtained solution was transferred into Teflon-lined autoclave and treated at 185°C for 36 h. The autoclave was cooled down to room temperature naturally, and the precipitates were collected and washed by absolute ethanol and distilled water. After dried through a freeze-drying process, the O-MoS₂/HN-CNFs was obtained. As the comparisons, the P-MoS₂/HN-CNFs was synthesized by directly thermal treatment of O-MoS₂/HN-CNFs under 500°C for 2 h in H₂/Ar flow. Moreover, compared with O-MoS₂/HN-CNFs, the O-MoS₂/N-C was prepared under the same conditions except the PPy was not coated on the surface of Mo-MOFs.

Structure Characterizations.

XRD patterns were measured by the instrument of PANalytical X'Pert PRO with Cu K α radiation ($\lambda = 1.5418 \text{ \AA}$) at 40 kV and 40 mA. The morphology and structure were characterized by scanning electron microscope (Hitachi SU8010, 15 kV) and transmission electron microscopy (Tecnai G² F30, 300 kV). X-ray photoelectron spectroscopy and Raman spectra analyses were carried out by using a spectrometer with Al K α radiation (Nepean, ON) and Renishaw INVIA. BET surface area and pore size distribution were characterized by the Micromeritics ASAP 2020.

Electrochemical Measurements.

The electrochemical performance of O-MoS₂/HN-CNFs, P-MoS₂/HN-CNFs, and O-

MoS₂/HN-C were investigated by a two-electrode configuration, and the CR2025-type coin cells were assembled in an argon-filled glove box with moisture and oxygen level <0.1 ppm. The cathode, anode, and separator of a coin cell are the as-prepared material, polished Mg plate, and microporous membrane (Celgard 2400). Moreover, the working electrodes were composed of 80 wt% active material, 10 wt% acetylene black, and 10 wt% polyvinylidene difluoride (PVDF). The forming homogeneous slurry coated on the carbon fiber paper with the loading of 1.0 mg cm⁻². All-phenyl complex (APC)+lithium chloride (LiCl) electrolyte for LMIBs was prepared as follows: 0.25 M aluminium chloride (AlCl₃) was slowly added to 20 mL anhydrous tetrahydrofuran (THF) solution and vigorous stirring for 12 h, and then 2.0 M phenyl magnesium chloride (MgPhCl) solution in THF was added dropwise to form the APC electrolyte under vigorous stirring for another 12 h. After that, 1.0 M lithium chloride (LiCl) was added to the above solution to form the Li⁺/Mg²⁺ dual-salt electrolyte. For MIBs, the same proportion of APC electrolyte without LiCl was configured. Electrochemical impedance spectroscopy (EIS) was measured at a frequency between 0.1 Hz and 100 kHz.

Galvanostatic intermittent titration technique (GITT) is performed by the Neware system. The batteries were measured for 5 min discharge and 20 min relaxing time at the current density of 50 mA g⁻¹. The diffusion coefficient can be calculated by Fick's second law:

$$D = \frac{4}{\pi\tau} \left(\frac{m_B V_M}{M_B S} \right) \left(\frac{\Delta E_s}{\Delta E_t} \right) \quad (1)$$

where τ is the time of current pulse, m_B , M_B , and V_M , are the mass, molar mass, and molar volume of active materials, respectively, S is the contact area of electrode/electrolyte. ΔE_s and ΔE_t are the steady-state potential change by the current pulse and potential change during the constant current, which are eliminated with the IR drop.

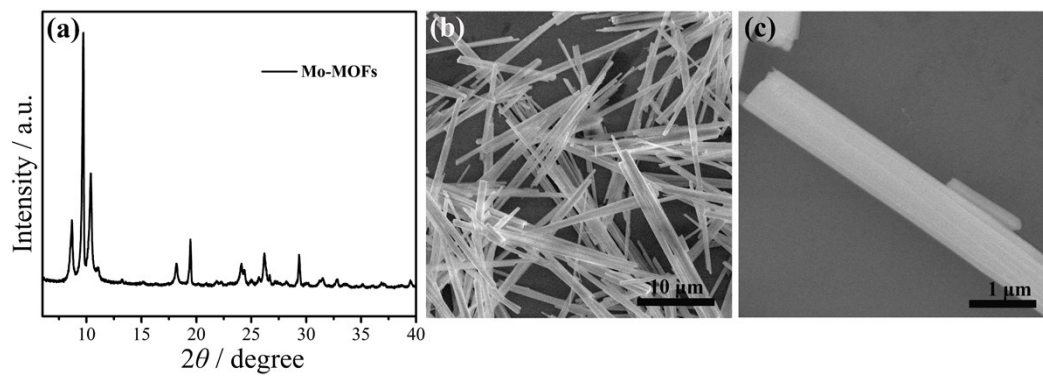


Fig. S1 (a) XRD pattern and (b, c) SEM images of Mo-MOFs.

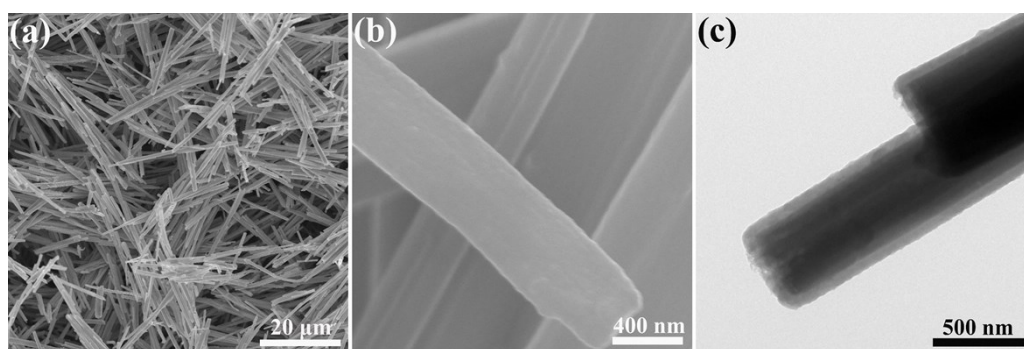


Fig. S2 (a,b) SEM and (c) TEM images of Mo-MOFs@PPy.

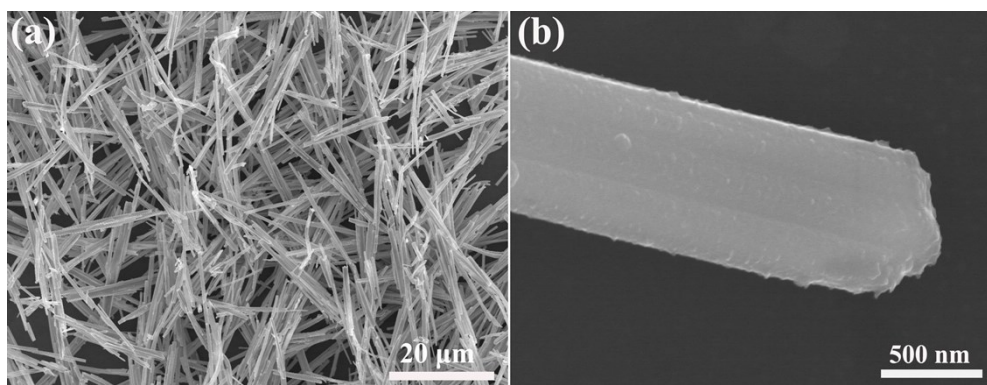


Fig. S3 (a,b) SEM images of Mo-precursor.

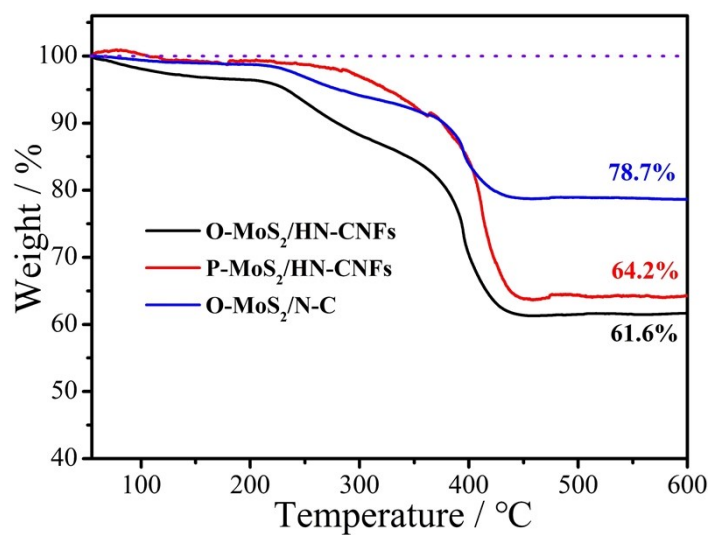


Fig. S4 TGA curves of O-MoS₂/HN-CNFs, P-MoS₂/HN-CNFs, and O-MoS₂/N-C.

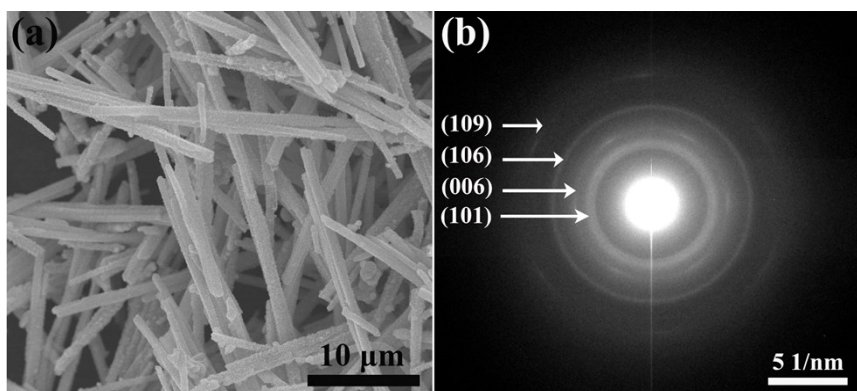


Fig. S5 (a) SEM image and (b) selected area electron diffraction pattern of O-MoS₂/HN-CNFs.

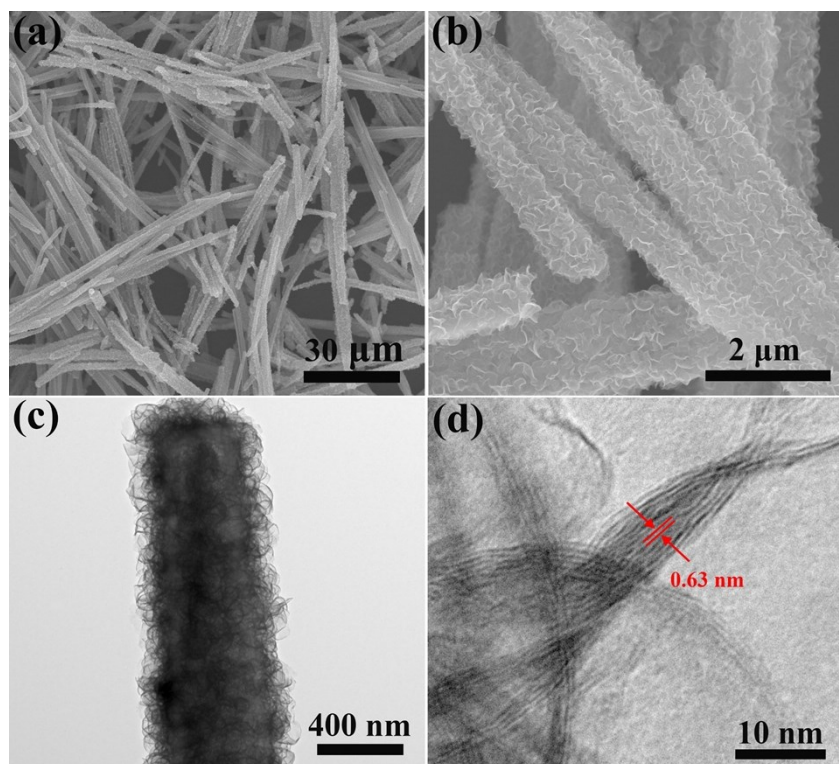


Fig. S6 (a,b) SEM,(c) TEM, and (d) HRTEM images of P-MoS₂/HN-CNFs.

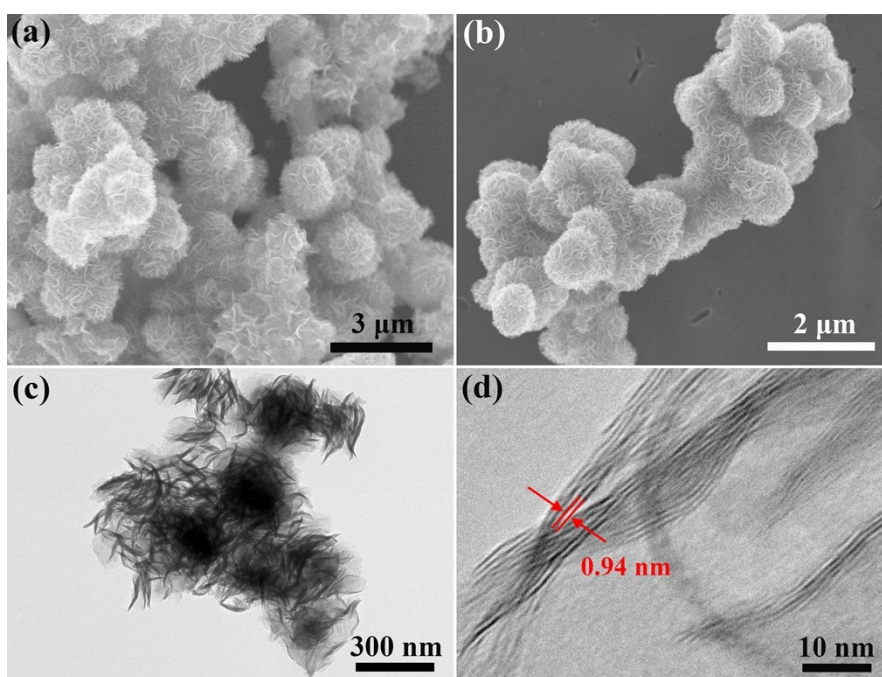


Fig. S7 (a,b) SEM,(c) TEM, and (d) HRTEM images of O-MoS₂/N-C.

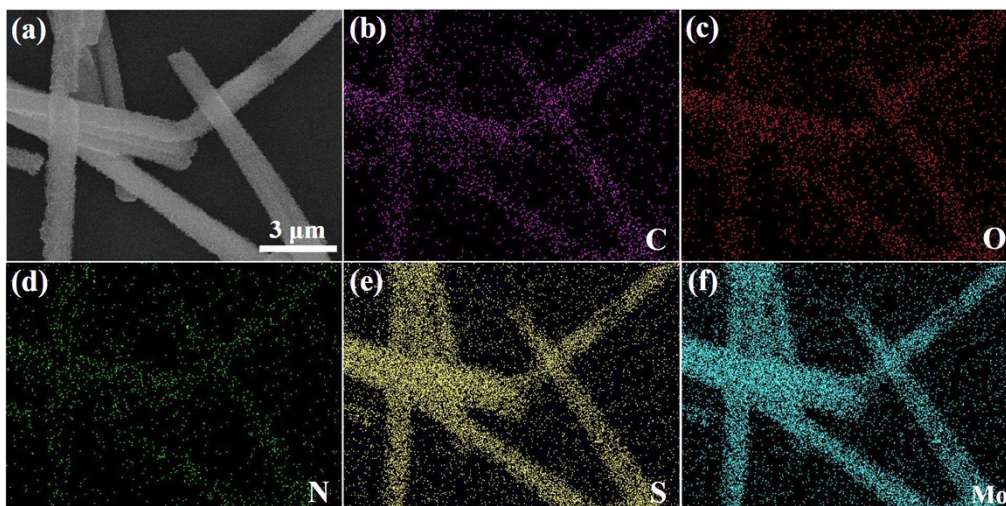


Fig. S8 (a–f) EDS elemental mapping images of C, O, N, S, and Mo for O-MoS₂/HN-CNFs.

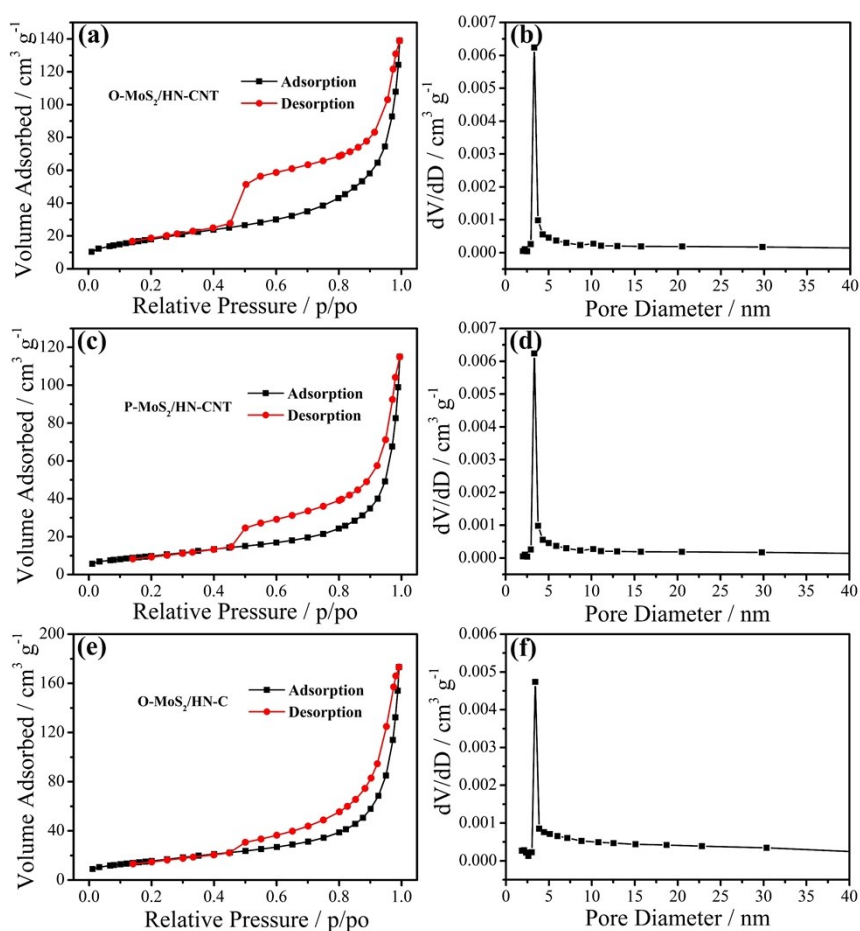


Fig. S9 (a, c, and e) Nitrogen adsorption and desorption isotherms and (b, d, and f) the corresponding pore-size distribution calculated of O-MoS₂/HN-CNFs, P-MoS₂/HN-CNFs, and O-MoS₂/N-C.

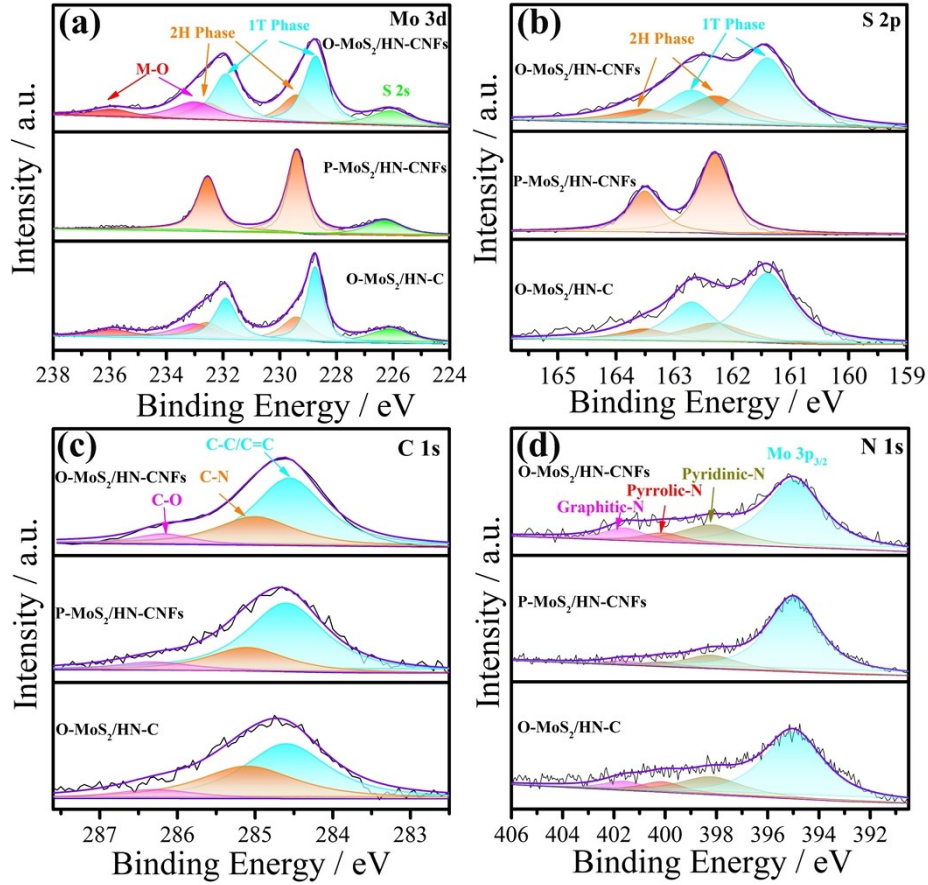


Fig. S10 XPS spectra of (a) Mo 3d, (b) S 2p, (c) C 1s, and (d) N 1s of O-MoS₂/HN-CNFs, P-MoS₂/HN-CNFs, and O-MoS₂/N-C.

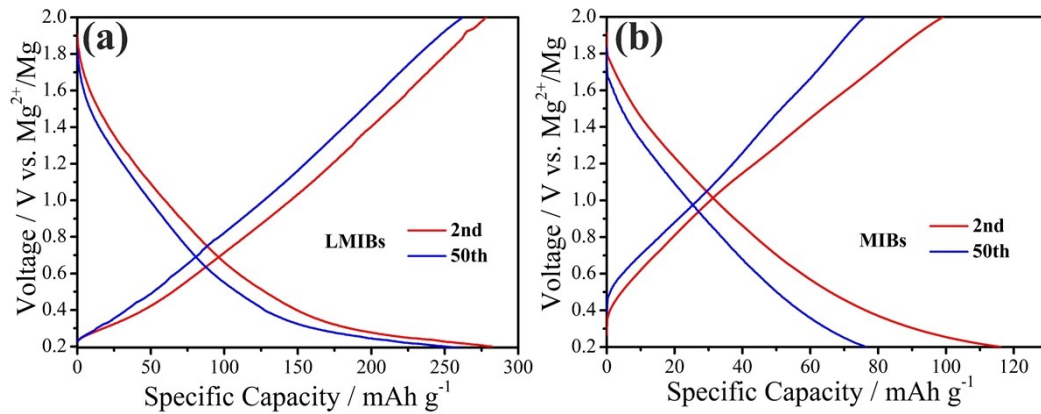


Fig. S11 Galvanostatic discharge-charge curves of O-MoS₂/HN-CNFs for (a) LMIBs and (b) MIBs.

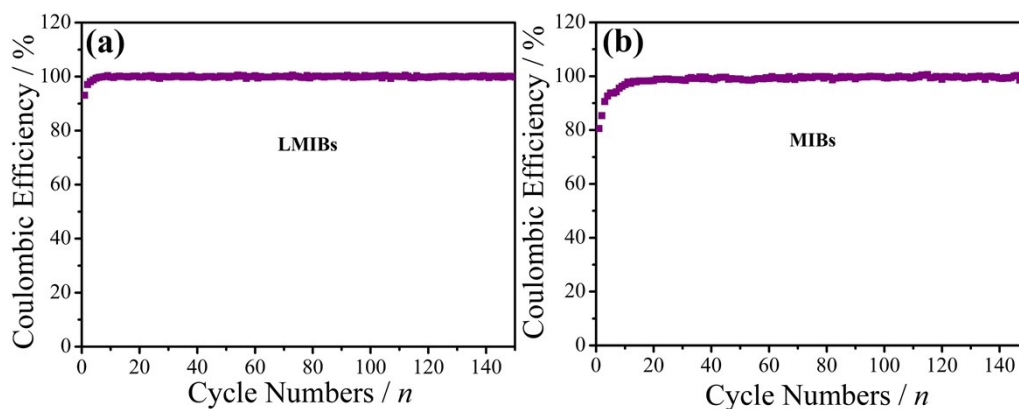


Fig. S12 Coulombic efficiency curves of O-MoS₂/HN-CNFs for (a) LMIBs and (b) MIBs.

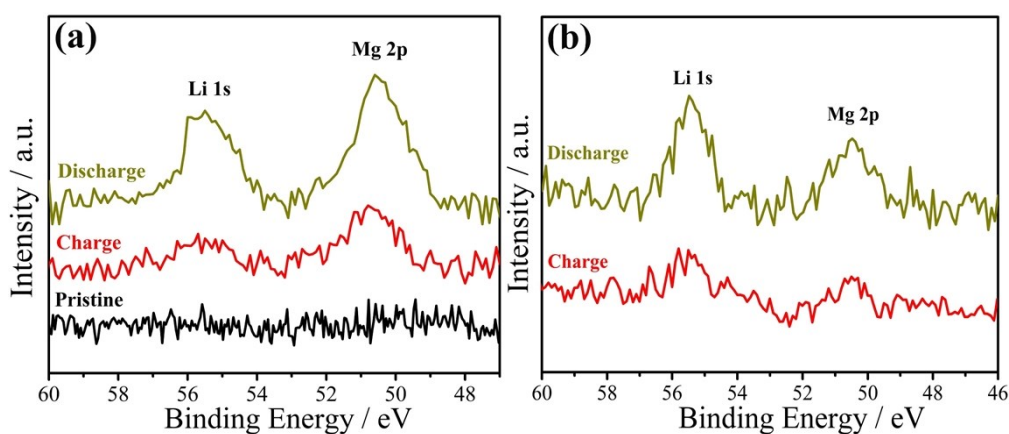


Fig. S13 XPS spectra of Li 1s and Mg 2p for O-MoS₂/HN-CNFs after 10th discharge and 11th charge processes at (a) 20 mA g⁻¹ and (b) 1000 mA g⁻¹.

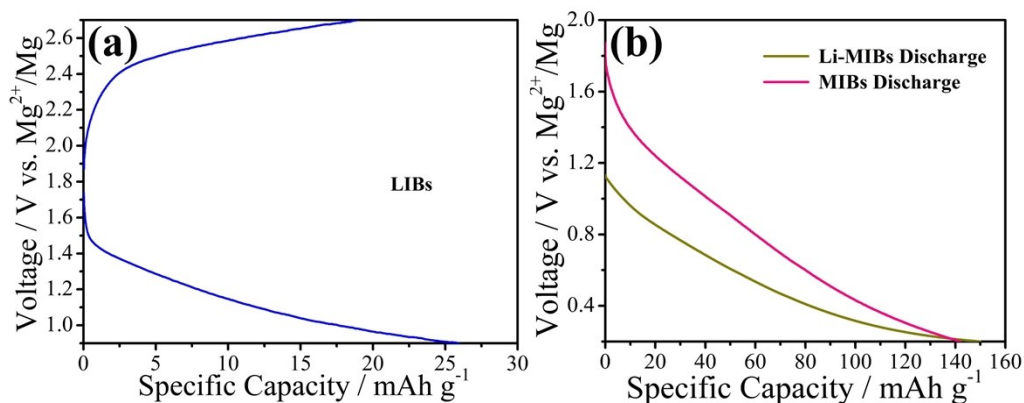


Fig. S14 (a) Galvanostatic discharge-charge curves for LIBs. (b) Discharge curves of Li-MIBs and MIBs.

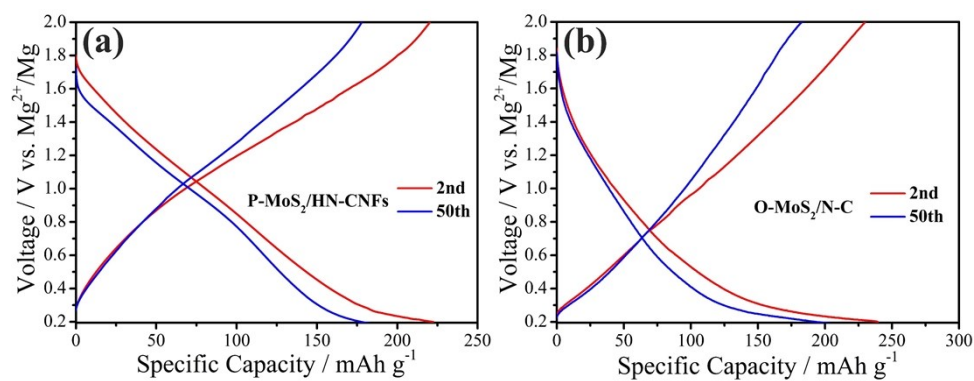


Fig. S15 Galvanostatic discharge-charge curves of (a) P-MoS₂/HN-CNFs and (b) O-MoS₂/N-C.

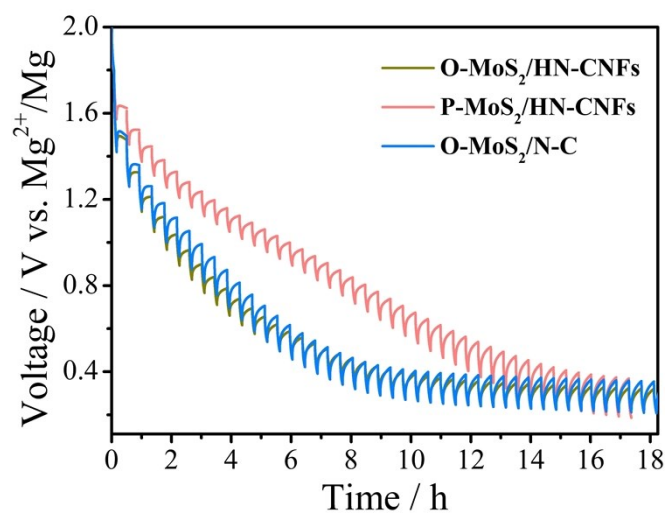


Fig. S16 GITT profiles of the discharge process of O-MoS₂/HN-CNFs, P-MoS₂/HN-CNFs, and O-MoS₂/N-C.

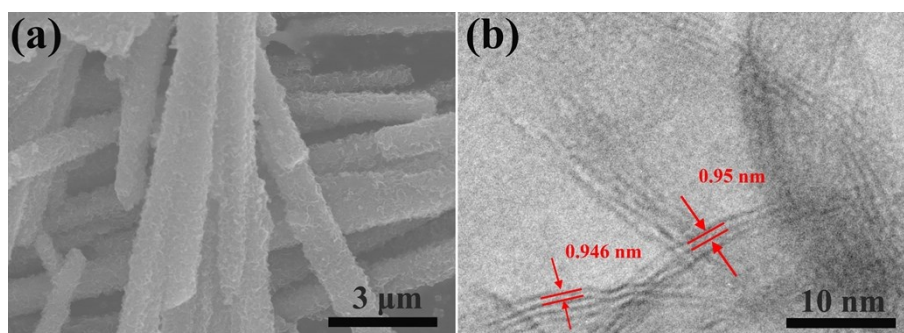


Fig. S17 SEM and HRTEM images of O-MoS₂/HN-CNFs after 100 cycles charge-discharge processes.

Table S1. Comparison of electrochemical performance of O-MoS₂/HN-CNFs with the previously reported cathode materials for LMIBs.

Electrode material	Current Density (mA g ⁻¹)	Reversible Capacity (mAh g ⁻¹)	Cycle Numbers (<i>n</i>)	Whether Li ⁺ /Mg ²⁺ Co-intercalation	Ref.
O-MoS ₂ /HN-CNFs	20 1000	249.2 134.4	150 2000	Yes	This work
Li ₃ V ₂ (PO ₄) ₃	100	135	200	No	<i>J. Mater. Chem. A</i> 2019, 7, 9968
VS ₂ -GO	90	200	100	No	<i>Energy Storage Mater.</i> 2018, 12, 61
V ₂ MoO ₈	20	135	50	Yes	<i>Nano Energy</i> 2017, 34, 26
Ti ₃ C ₂ T _x /CNT	100	~80	500	No	<i>ACS Appl. Mater. Interfaces</i> 2017, 9, 4296
V ₂ C MXene	50	~110	480	Yes	<i>Small</i> 2020, 16, 1906076
Cu ₂ Se	26	~110	30	No	<i>Electrochim. Acta</i> 2018, 261, 503
Cu ₂ Se/rGO	26	~65	100	No	
LiCrTiO ₄	20	~125	30	No	<i>Chem. Eur. J.</i> 2017, 23, 17935
TiS ₂	80	160	400	No	<i>Adv. Energy Mater.</i> 2015, 5, 1401507
Li ₄ Ti ₅ O ₁₂	60	~125	500	Yes	<i>Angew. Chem. Int. Ed.</i> 2015, 54, 5757
MoSe ₂ /C	200	89	100	No	<i>Electrochem. Commun.</i> 2018, 90, 16
VO ₂	20	154.9	100	No	<i>ACS Appl. Mater. Interfaces</i> 2017, 9, 17060